Available online at www.eccomasproceedia.org
Eccomas Proceedia COMPDYN (2019) 4115-4127

ECCOMAS
Proceedia

COMPDYN 2019
7th ECCOMAS Thematic Conference on
Computational Methods in Structural Dynamics and Earthquake Engineering
M. Papadrakakis, M. Fragiadakis (eds.)
Crete, Greece, 24–26 June 2019

SEISMIC SHEAR AND MOMENT DEMANDS IN REINFORCED CONCRETE WALL BUILDINGS

Alejandro Morales[1], Paola Ceresa[2], and Matías Hube[3]

[1] School of Civil Engineering - Universidad de Valparaíso
222 General Cruz Street, Valparaíso, Chile
e-mail: alejandro.morales@uv.cl

[2] Seismic Hazard and Risk Analysis, Risk Engineering and Development RED
(formerly at the University School for Advanced Studies Pavia – IUSS Pavia)
Via Frank, 38, 27100 Pavia, Italia
paola.ceresa@redrisk.com

[3] Department of Structural and Geotechnical Engineering - Pontificia Universidad Católica de Chile
4860 Vicuña Mackenna Avenue, Santiago, Chile
mhube@ing.puc.cl

Abstract

This research aims to obtain envelopes of the moment and shear demands in reinforced concrete (RC) wall buildings subjected to ground motions. These envelopes are intended to be used for designing RC buildings. Three research buildings with non-rectangular walls designed according to Eurocode 8 are considered. The seismic performance of the buildings is evaluated from nonlinear response history analysis (NRHA) with increasing levels of ground motion intensity. The RC walls are simulated with a model with distributed inelasticity (MDI), which considers that the nonlinear behaviour can take place at any building level if the demand is larger than the wall yield capacity, while the flexural stiffness is a function of the moment demand of the wall. The design envelopes for moment and shear forces are obtained from the results of the NRHA, where the effects of higher modes are evidenced.

Keywords: Reinforced concrete, Walls, Seismic demands, Seismic behaviour.

ISSN:2623-3347
Peer-review under responsibility of the organizing committee of COMPDYN 2019.
doi: 10.7712/120119.7211.20160

1 INTRODUCTION

In high seismicity areas, RC structural walls are largely used as lateral-load resisting systems for mid- and high-rise buildings. RC walls are stiff and strong, easily incorporated into architectural layouts, and, when properly designed and detailed, perform satisfactorily when subjected to severe earthquakes. Structural walls can be configured in numerous ways within a building, with multiple walls resisting the demands in each principal direction. Rectangular sections are relatively easy to be designed, and have been extensively studied in the last years. Intersecting wall segments can be combined to create flanged or non-rectangular walls, including T-, C-, and L-shaped cross sections. RC walls are common in residential buildings and hotels and are usually located around stairs, elevators, corridors, and partitions between residential units [1].

Seismic moment and shear forces demand in walls of RC buildings have been studied mainly using a single wall as a representation of the entire building, where the interaction between different walls within buildings is not considered [2, 3]. Moreover, these studies assume that the nonlinear behaviour takes place at the base of the wall only. Therefore, elements with lumped plasticity and constant stiffness above the critical section have been used. The first problem of this approach is that a constant flexural stiffness is considered along the wall height. However, the flexural stiffness of the wall is a function of the moment demand which varies along the wall height. A second problem of such approach, that assumes an elastic response above the critical section, is that the bending moments in such regions are not bounded, while the bending moment at the base is bounded by the provided moment strength. Because certain design codes specify design envelopes for bending moments in RC wall buildings (e.g. Eurocode 8, NZS 3101, CSA A23.3), the assumption of elastic response and unbounded bending moments above the base of the walls may be an unrealistic situation under severe earthquakes.

The main objective of this research is to provide design recommendations for RC wall buildings. Specifically, design envelopes for moment and shear demands are proposed. The envelopes are obtained from an analytical study of three research buildings with non-rectangular RC walls.

2 RESEARCH BUILDINGS

The plan view of the research buildings is shown in Figure 1, where T-shaped and C-shaped RC walls are considered to resist lateral loads in both directions. The buildings have ten, twenty and thirty storeys and the inter-storey height is 3.0 m. The thickness of the walls of the three buildings varies between 0.3 m and 0.4 m, depending on the number of storeys.

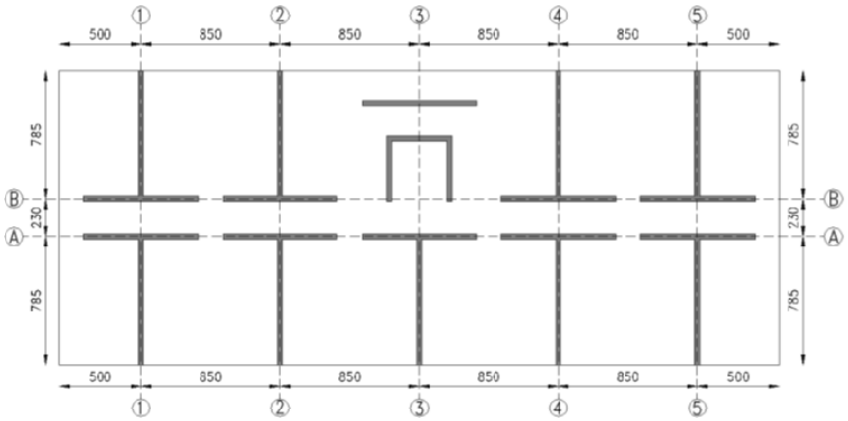

Figure 1: Plan view of the research buildings (dimensions in centimetres).

The buildings were designed according to Eurocode 8 (EC8) [4]. A type C soil (dense sand or gravel, or stiff clay) was used in conjunction with 0.4g design ground acceleration, considering a high seismicity area. The properties of concrete and reinforcement adopted for the seismic design are typical values used in engineering practice. The yield strength of the reinforcement (f_y) and characteristic compressive strength of the concrete (f'_c) are 500 MPa and 30 MPa, respectively.

Table 1 summarises the main design outputs of the three buildings, where T is the fundamental period of the buildings, q is the behaviour factor for uncoupled wall systems of high ductility class [4], W is the seismic weight, V is the design base shear of the building, ρ_L is the longitudinal reinforcement ratio, N_{ed} is the factored axial load in the walls, and A_g is the gross area of the walls. The value of ρ_L for the 30-storey building is lesser than that the 20-storey one because of the lower seismic demand induced by the larger period of the tall building.

N°-Storey	T [sec]	q	W [kN]	V/W	T-shaped wall		C-shaped wall	
					ρ_L [%]	$N_{ed}/A_g f'_c$	ρ_L [%]	$N_{ed}/A_g f'_c$
10-Storey	0.45	4.4	73412	0.19	0.5	0.06	0.6	0.05
20-Storey	1.12	4.4	156108	0.11	0.8	0.11	0.7	0.10
30-Storey	2.40	4.4	252851	0.08	0.7	0.15	0.4	0.16

Table 1: Design outputs.

3 ANALYTICAL MODELS OF BUILDINGS

The seismic performance of the research buildings is estimated from two-dimensional (2D) nonlinear response history analyses (NRHA) using the finite-element software RUAUMOKO 2D [5]. The walls and beams are modelled using beam elements with lumped flexural nonlinear behaviour and elastic shear behaviour.

Figure 2 shows the two-component beam element used to model the walls, where two members in parallel represent the behaviour of the element. The two members are elastic but one of them allows the formation of hinges at ends of the member [5]. The nonlinear behaviour is achieved assigning a hysteretic model to the flexural behaviour of the hinges.

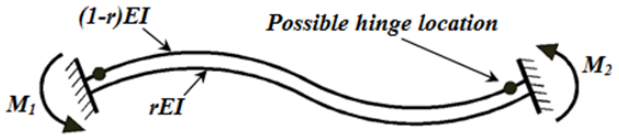

Figure 2: Two-component beam element, adapted from Carr [5].

In this study, the nonlinear moment-rotation relationship of the hinges of the two-component beam elements used to represent the RC walls is represented using the tri-linear SINA hysteretic model [6]. This hysteretic model is shown in Figure 3a and consists on a tri-linear backbone with stiffness changes at cracking (F_{cr}^+, F_{cr}^-) and yielding (F_y^+, F_y^-). The SINA hysteresis rule allows different behaviour in the two loading directions, allowing modelling the behaviour of asymmetric RC walls. Additionally, the pinching effect is considered through the definition of the crack closing moment (F_{cc}). The SINA model considers that F_{cc} is the same in both directions.

Using available experimental data of non-rectangular RC walls subjected to cyclic loads reported by Thomsen and Wallace [7] (named TW1, TW2), Sittipunt and Wood [8] (CLS, CMS), Beyer et al. [9] (TUA, TUB), and Brueggen [10] (NTW1, NTW2), the RC wall model

was calibrated achieving a good representation of the cyclic behaviour of the tested walls. For each specimen the tri-linear backbone was obtained directly from the moment-curvature relationship while the crack closing moment (F_{cc}) was defined through a trial and error procedure. The values of F_{cc} obtained for the specimens are shown in Figure 3b. The comparison between the experimental behaviour and the predicted response for two specimens is shown in Figure 4, where the proposed model is able to predict the cyclic response adequately in both loading directions.

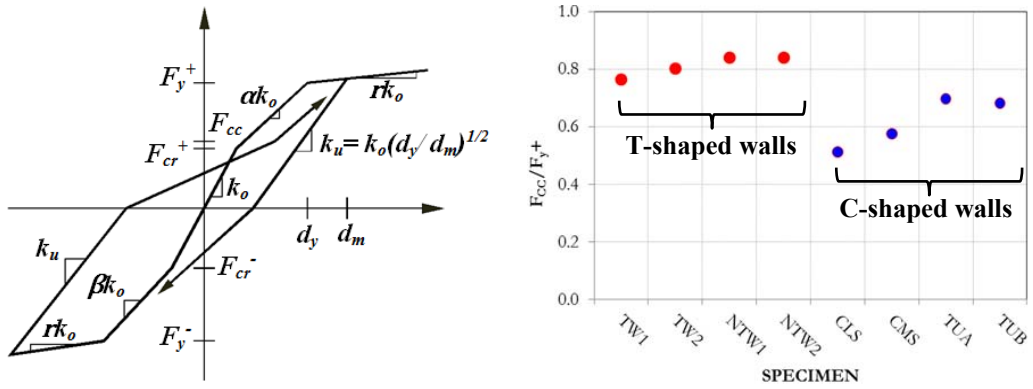

a) b)

Figure 3: a) Tri-linear SINA hysteretic model, adapted from Carr [5], and b) F_{cc} values used for the studied walls.

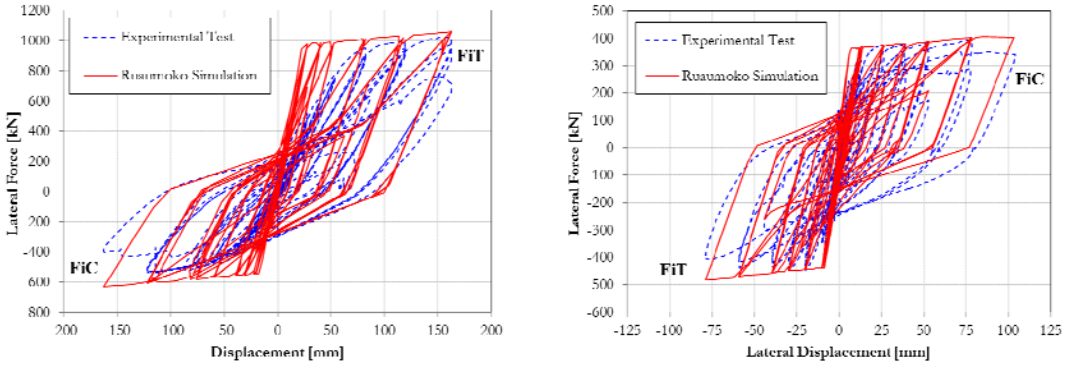

a) b)

Figure 4: Comparison between the analytical model and experimental results: a) T-shaped wall (NTW1) after Brueggen [10], and b) C-shaped wall (TUA) after Beyer et al. [9].

Figure 4 shows that the experimental yield displacements, mainly for flange in tension (FiT), are larger than the analytical values due to the gradual yielding of the tension reinforcement within the flanges, whereas the reinforcement closest to the webs yields first, and subsequently progressing out from the web–flange intersection as lateral displacement increases [11]. Even though the simulated values overestimate the elastic stiffness, the proposed model is considered adequate because the response of the studied walls is essentially inelastic.

3.1 Building Model

The two-dimensional model of the building is shown in Figure 5, where all the axes of the building are modelled simultaneously. The walls were modelled with two-components beam elements using the described tri-linear SINA hysteretic constitutive relationship that considers different strength and stiffness in opposite directions. The effective slabs, which connect the

two walls in each axis, were modelled using two-node beam elements considering the Takeda hysteretic rule. End offsets are considered in these elements to account for the wall widths.

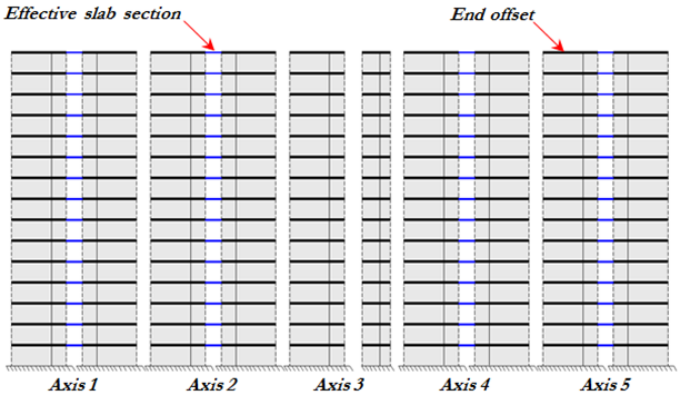

Figure 5: RUAUMOKO 2D structural model of studied buildings.

To model the RC walls, the approach used in this study is a model with distributed inelasticity (MDI), which considers that the nonlinear behaviour can take place anywhere in the wall if the moment demand is larger than the yield moment. The MDI of one wall is shown in Figure 6a, where four two-component beam elements are considered at each storey. This number of elements is considered adequate to represent satisfactorily the lateral displacement profile and flexural lateral stiffness of the walls. Since the inelastic behaviour is lumped in discrete points along the wall height (perfect hinge of two-component beam element), the proposed model in RUAUMOKO 2D was validated with a fibre beam model developed with SeismoStruct [12]. The comparison of a static pushover analysis of the T-shaped wall predicted with the two models in both loading directions is shown in Figure 6b. For the pushover analysis a concentrated load at the top of the wall was considered. The figure shows that the obtained behaviour with both models is similar for the two loading directions (flange in compression (FiC) and flange in tension (FiT)). Therefore, the proposed model with two-component beam elements is able to predict the behaviour of the wall adequately. A further development of the research will be the validation of the proposed MDI model with a fibre beam-column element able to capture the nonlinear shear behaviour of the wall [13, 14] and the multi-axial stress interaction under multi-axial loading conditions [15, 16].

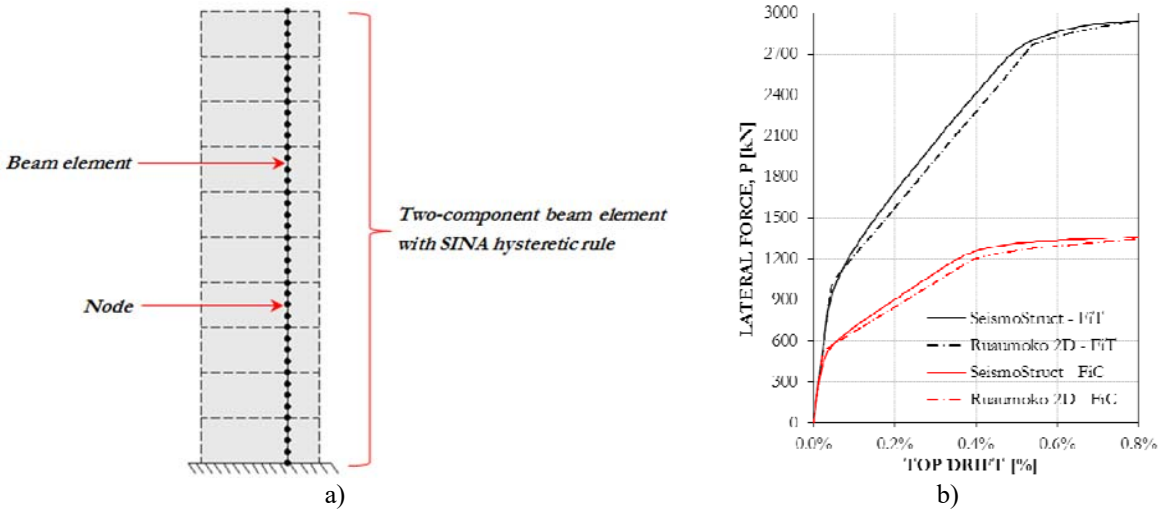

Figure 6: a) MDI and b) comparison of pushover analysis of the T-shaped wall using the proposed model with Ruamoko 2D and a fiber model with SeismoStruct.

4 CONSIDERED GROUND MOTIONS

To carry out the NRHA of the three buildings (Table 1) a set of seven artificial accelerograms were generated to be compatible with the design spectrum of EC8 [4]. Artificial records were selected because they matched the design spectrum for almost the full period range with a comparatively small error. The number of records was selected according to the prescriptions of the design codes (IBC, EC8, among others), which prescribe a minimum of seven spectrum-compatible records in order to obtain representative average results for design verification. The accelerograms were generated with SeismoArtif v2016 program [17]. Figure 7 compares the pseudo-acceleration and displacement spectra for 5% damping for each accelerogram with those of the EC8 design spectrum. Additionally, the figure shows the average response spectrum of the artificial accelerograms.

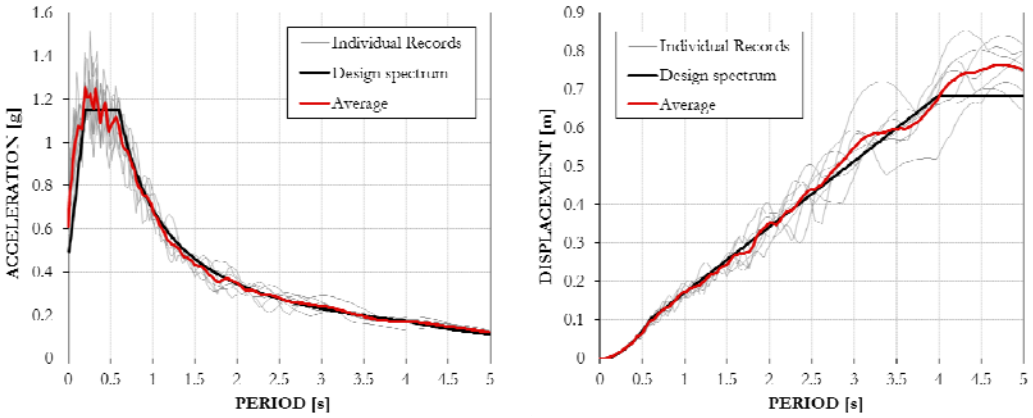

a) b)

Figure 7: EC8 design and artificial spectra used for NRHA: a) pseudo-acceleration and b) displacement.

5 RESULTS

The results obtained from NRHA are presented in this Section. The NRHAs were performed with RUAUMOKO 2D program using the seven records mentioned in the previous section. The records were scaled to 100% (IR=1.0), 150% (IR=1.5) and 200% (IR=2.0) of the design intensity to analyze the seismic behaviour of the buildings. The use of seven records for each analysis permits to obtain representative average values of the moments and shear forces.

From the nonlinear results of the buildings, moments and shear design envelopes are proposed for the walls of the studied buildings with the non-rectangular walls. Figure 8 shows the shape of the moment and shear envelopes and the parameters that define them (whose definition will be given later).

The proposed envelopes for capacity design are based on the Simplified Capacity Design model for rectangular cantilever RC walls developed by Priestley et al. [18]. This model was also used on T-shaped walls by Smyrou et al. [19]. However, the results obtained in this study present several differences with respect to the previous ones, as it is explained in the following sections.

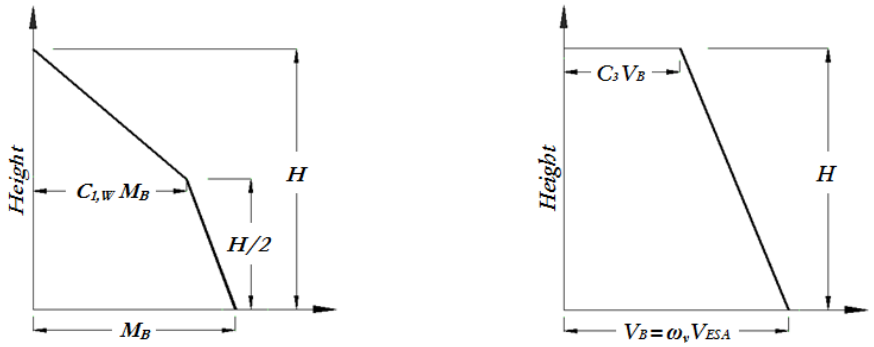

a) b)

Figure 8: Capacity design envelope for cantilever walls: a) moment and b) shear.

5.1 Superposition of the proposed envelopes and demands from NRHA

Figures 9, 10 and 11 show the maximum moment and shear demands from the NRHA, its average values and the proposed design envelopes (moment and shear forces). Due to the limited space, only some representative results are presented in this paper; however, more information is available elsewhere [20]. As expected, the figures shown different responses of the walls for the flange in tension (FiT) and flange in compression (FiC) directions, which is an important difference with respect to the responses of rectangular walls.

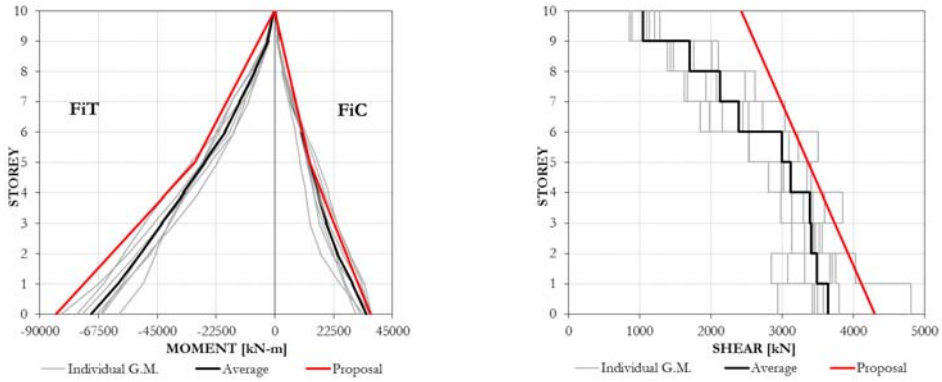

a) b)

Figure 9: T-shaped wall demands and design envelopes for 10-storey building (IR=1.0): a) moment and b) shear force.

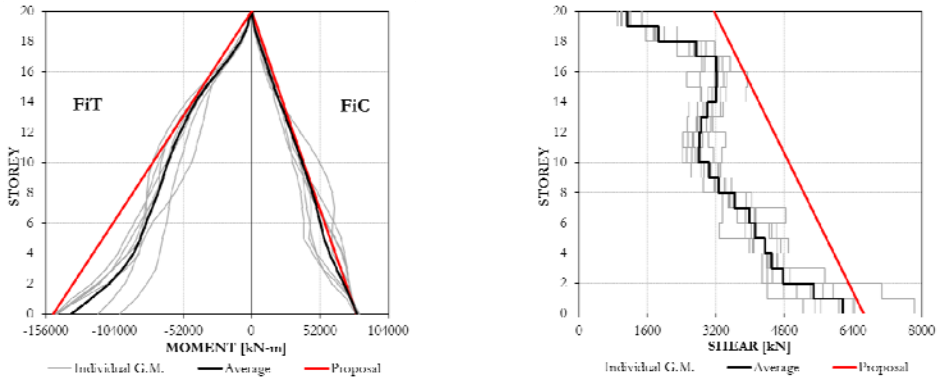

a) b)

Figure 10: T-shaped wall demands and design envelopes for 20-storey building (IR=1.5): a) moment and b) shear force.

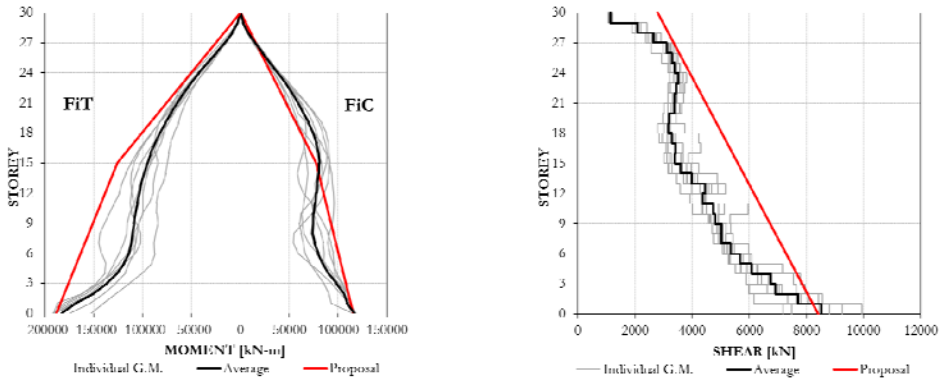

a) b)

Figure 11: T-shaped wall demands and design envelopes for 30-storey building (IR=2.0): a) moment and b) shear force.

5.2 Moment envelope

Figure 12 shows the values of the $C_{1,W}$ coefficient estimated for each record and each seismic intensity for the 10-storey building. This coefficient is the ratio of the mid-height moment to the overstrength base moment M_B (see Figure 8) that considers the overstrength conditions at the base hinge (strain hardening of reinforcement). The $C_{1,W}$ coefficients are similar for FiC and FiT for each intensity level; however, a large number of analyses is necessary to estimate the relationship between the storey numbers (or elastic period), the intensity ratio (IR) and the $C_{1,W}$ coefficient.

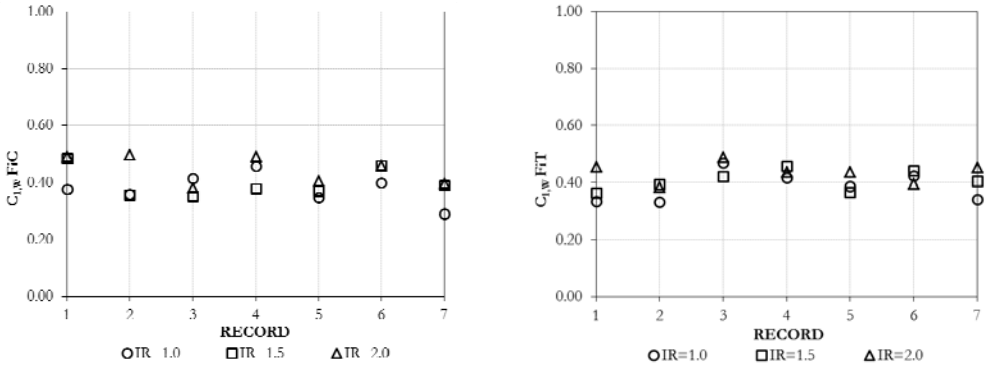

a) b)

Figure 12: Ratio of mid-height moment over base moment for T-shaped wall of 10-storey building with different intensity levels: (a) FiC, and (b) FiT.

The $C_{1,W}$ coefficients obtained for the three research buildings and three seismic intensity ratios (IR) are summarized in Table 2. The results obtained in this work show that the dynamic amplification in moment and shear profiles increases for higher intensity. The same tendency has been demonstrated in previous studies of RC wall buildings [3, 18, 19]. Therefore, the moment and shear force envelopes need to be related to the seismic intensity, which is characterized by the curvature ductility demand (μ_Φ) due its direct relationship with the seismic intensity.

N°-Storey	$C_{1,W\ FiC}$			$C_{1,W\ FiT}$		
	IR=1.0	IR=1.5	IR=2.0	IR=1.0	IR=1.5	IR=2.0
10-Storey	0.38	0.40	0.45	0.39	0.41	0.44
20-Storey	0.36	0.48	0.56	0.46	0.46	0.51
30-Storey	0.44	0.58	0.69	0.52	0.50	0.52

Table 2: Summary of $C_{1,W}$ coefficients.

From the $C_{1,W}$ values for FiC the following equation is proposed, which can also be conservatively be used for FiT.

$$C_{1,W} = m\,\mu_\Phi + b \tag{1}$$

where μ_Φ is the curvature ductility demand for FiC at the base of the walls, while the coefficient m and b are given by Equation 2 and Equation 3, respectively. These latter coefficients, estimated with a regression analysis, depend on the elastic periods of the buildings (T_e).

$$m = 0.022\,T_e + 0.006 \tag{2}$$

$$b = 0.03\,T_e + 0.33 \tag{3}$$

For the calibration and definition of previous equations, which define the moment and shear envelopes, the curvature ductility demand for FiC was used, even though the response of the T-shaped walls was different for FiT and FiC. For FiC both stiffness and yield curvature are lesser than for FiT. Therefore, due to the fact that larger nonlinear behaviour (or ductility demand) is expected if the flange acts in compression, the use of the curvature ductility demand for FiC is justified.

5.3 Shear envelope

NRHAs indicate that the shear force demand in the T-shaped walls is larger for the direction with FiT than for that with FiC because the moment strength and the stiffness of the wall is larger for the direction with FiC. Figure 13 shows the coefficient ω_v for the 10-storey building. This coefficient is the ratio of the maximum shear forces from NRHA at the base (V_B) to the shear forces from an equivalent static analysis (V_{ESA}), the capacity design base shear is calculated as the product of V_{ESA} at the base and ω_v (see Figure 8b). To estimate the base shear force of the wall (V_{ESA}) the provided moment strength at the base of the wall should be considered. Table 3 summarizes the maximum shear forces and the amplification factors (ω_v) for the three research buildings and three seismic intensity ratios (IR). The table shows that the values of ω_v depend on the seismic intensity, storey number, and the loading direction (FiC or FiT). Table 3 summarises the maximum average values for base shear forces from NRHA and equivalent static analysis, for T-shaped walls when flange acts in compression (FiC) and tension (FiT). Since the shear is resisted mostly by the web of the walls, identifying the loading direction is not relevant to the definition of the envelope, but the estimation of the ω_v factor should be consistent with the direction of analysis. In this study, the amplification factors ω_v were calculated with the shear forces for FiT. Table 3 shows that ω_v increases with the storey

numbers and with the seismic intensity. Therefore, this amplification factor increases with the elastic period (T_e) and curvature ductility demand (μ_Φ).

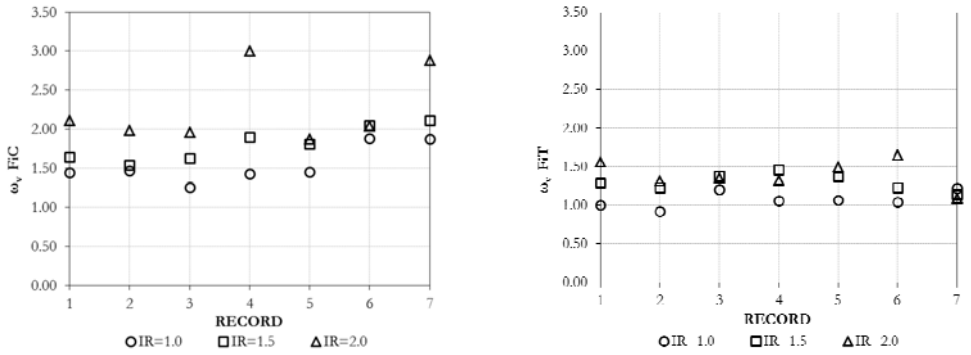

a) b)

Figure 13: Ratio between base shear from NRHA and ESA for T-shaped wall of 10-storey building with different intensity levels: (a) FiC, and (b) FiT.

N°-Storey	IR	Moment [kN-m]		Shear forces [kN]				ωv
		$M_{B\ FiC}$	$M_{B\ FiT}$	$V_{ESA\ FiC}$	$V_{ESA\ FiT}$	$V_{B\ FiC}$	$V_{B\ FiT}$	
10-Storey	1.0	34900	-70173	1685	3389	2579	-3641	1.07
	1.5	38609	-84406	1865	4076	3371	-5283	1.30
	2.0	41260	-87291	1993	4216	4482	-5903	1.40
20-Storey	1.0	65881	-105189	1624	2592	3402	-4226	1.64
	1.5	79981	-137129	1971	3380	4892	-5898	1.75
	2.0	83791	-149043	2065	3673	5672	-7804	2.12
30-Storey	1.0	90407	-128457	1494	2122	4776	-4387	2.06
	1.5	113071	-167429	1868	2766	5790	-7329	2.65
	2.0	116621	-183336	1927	3029	6824	-8060	2.68

Table 3: Summary of maximum shear forces and amplification factors.

From the ω_v values for FiT, the following equation is proposed.

$$\omega_v = 0.10\mu_\Phi + 0.5T_e + 0.70 \quad (4)$$

The ratio between the base shear and the top shear of the wall is given by:

$$C_3 = -0.08T_e + 0.60 \quad (5)$$

In previous equations, the curvature ductility demand for FiC and the elastic period of the building were used.

5.4 Comparison with previous studies

This section compares the proposed moment and shear design envelopes with those proposed by Priestley et al. [18] and Smyrou et al. [19]. Figure 14 compares the ratio of the mid-height moment over the base moment for the three research buildings. The model of Smyrou et al. is the most conservative for all the research buildings. On the other hand, for the 10-storey building, the ratios of the proposed model are similar to the ones of Priestley et al. approach. However, for taller buildings and larger ductility demands the aforementioned tendency changes and the values obtained from the proposed model are larger than those proposed by Priestley et al.

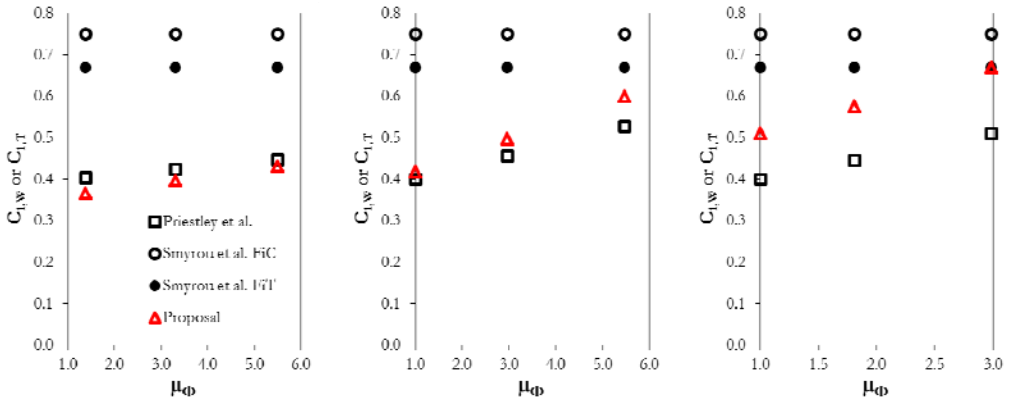

Figure 14: Ratios of mid-height moment over the base moment according to different approaches: a) 10-storey building, b) 20-storey building, and c) 30-storey building.

Figure 15 compares the dynamic amplification factors (ω_v) obtained from the proposed model with those presented by for Smyrou et al. and Priestley et al. for the three buildings. For the 10-storey building, the amplification factors of the proposed model are significantly larger than those of the other two models. For the 20- and 30-storey building, despite the differences between the models are lesser, the proposed approach is more conservative.

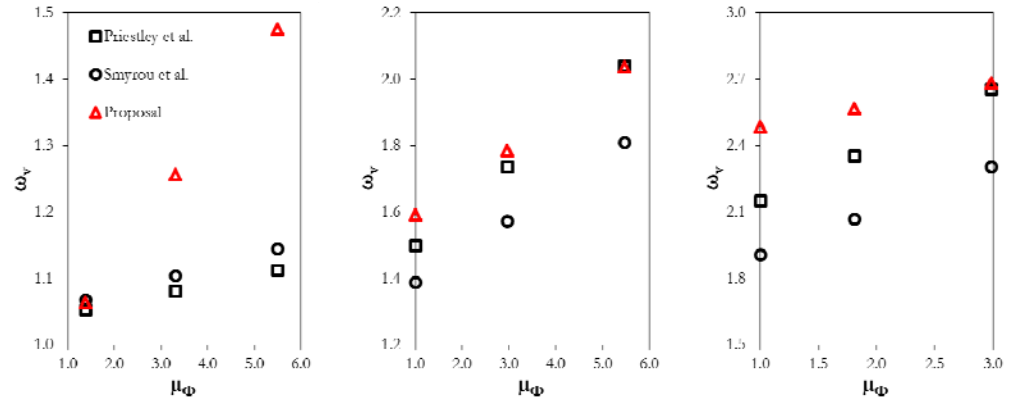

Figure 15: Dynamic amplification factors according to different approaches: a) 10-storey building, b) 20-storey building, and c) 30-storey building.

The discrepancies between the proposed model and the other two studied models can be explained by the different assumptions used in each of the cases. The periods of the studied

buildings are significantly smaller than those of the buildings studied by Priestley et al. and Smyrou et al. The larger periods of the buildings studied by Priestly et al. are related to the use of the direct displacement-based seismic design (DDBD) approach for designing their buildings. In this study, the EC8 design code was used, which resulted in buildings with shorter periods because of the drift limitation of the code. Another difference is that the flexural stiffness considered in this study varies along the height of the buildings due to the variation of the axial load in the walls (or moment strength) and also varies for FiC and FiT, whereas the flexural stiffness considered by Smyrou et al. and Priestley et al. was considered constant above the critical section.

Finally, in this study the whole building was modelled, which is expected to capture the interaction between walls [21].

6 CONCLUSIONS

In this work, three RC buildings with non-rectangular walls were designed according to Eurocode 8 and their seismic performance was assessed from nonlinear response history analysis (NRHA) for three different ground motion intensity levels. Walls were modelled with a model with distributed inelasticity (MDI) and the nonlinear behaviour was represented with a calibrated hysteretic rule. Capacity design envelopes for moment and shear of RC walls are proposed as a function of the building elastic period and the wall curvature ductility demand. These envelopes were defined and calibrated from the results of NRHA on T-shaped walls using a MDI. The proposed design envelopes have differences with respect to previous ones available in the literature. The differences are related to the use of non-rectangular walls in this study where strength and stiffness depend on the direction of loading. Additionally, this study considered the entire building in the analysis model, capturing the interaction and redistribution of strength between the walls within of building. The proposed envelopes are intended to be used for designing RC buildings.

7 ACKNOWLEDGMENTS

The first author acknowledges the support of the Becas Chile Programme (CONICYT) in form of PhD scholarship.

REFERENCES

[1] J. Moehle, *Seismic design of reinforced concrete buildings*. McGraw-Hill Education, New York, 2015.

[2] D. Pennucci, T.J. Sullivan, G.M. Calvi, Inelastic higher-mode response in reinforced concrete wall structures. *Earthquake Spectra*, **31**, 1493-1514, 2015.

[3] N. Priestley, A. Amaris, *Dynamic amplification of seismic moments and shear forces in cantilever walls. Research Report ROSE – 2002/01*. IUSS press, Pavia, Italy, 2002.

[4] CEN, *Eurocode 8 – Design of structures for earthquake resistance- Part 1: General rules, seismic actions and rules for buildings, EN 1998-1*. European Committee for Standardization, Brussels, Belgium, 2004.

[5] A.J. Carr, *Ruaumoko Manual – Volume 3: User manual for the 3-dimensional version Ruaumoko3D*. Department of Civil Engineering, University of Canterbury, Christchurch, New Zealand, 2012.

[6] M. Saiidi, M. Sozen, *Simple and complex model for nonlinear seismic response of reinforced concrete structures. A Report to the National Science Foundation*. Research Grant PFR 78-16318, 1979.

[7] J.H. Thomsen, J.W. Wallace, *Displacement-Based Design of RC Structural Walls: Experimental Studies of Walls with Rectangular and T-shaped Cross Sections. Report No.CU/CEE-95/96.* Department of Civil and Environmental Engineering, Clarkson University, 1995.

[8] C. Sittipunt, S. Wood, *Finite Element Analysis of Reinforced Concrete Shear Walls. A Report to the National Science Foundation*. Research Grant BCS 89-12992, 1993.

[9] K. Beyer, A. Dazio, M.J.N. Priestley, Quasi-static cyclic tests of two U-shaped reinforced concrete walls. *Journal of Earthquake Engineering*, **12**, 1023-1053, 2008.

[10] B.L. Brueggen, *Performance of T-shaped Reinforced Concrete Structural Walls under Multi-Directional Loading*. Ph.D Thesis, University of Minnesota, 2009.

[11] J.H. Thomsen, J.W. Wallace, Displacement-based design of slender reinforced concrete structural walls – experimental verification. *Journal of Structural Engineering*, *ASCE*, **130**, 618-630, 2004.

[12] Seismosoft, *SeismoStruct v6.5 – A computer program for static and dynamic nonlinear analysis of framed structures*. Available from http://www.seismosoft.com, 2013.

[13] A. Kagermanov, P. Ceresa, Physically Based Cyclic Tensile Model for RC Membrane Elements, *Journal of Structural Engineering, ASCE*, **142**(12), https://doi.org/10.1061/(ASCE)ST.1943-541X.0001590, 2016.

[14] A. Kagermanov, P. Ceresa, Fiber-Section Model with an Exact Shear Strain Profile for Two-Dimensional RC Frame Structures, *Journal of Structural Engineering, ASCE*, **143** (10), https://doi.org/10.1061/(ASCE)ST.1943-541X.0001839, 2017.

[15] A. Kagermanov, P. Ceresa, RC Fiber-Based Beam-Column Element with Flexure-Shear-Torsion Interaction. In: Hordijk D., Luković M. (eds) *High Tech Concrete: Where Technology and Engineering Meet*. Springer, Cham, https://doi.org/10.1007/978-3-319-59471-2_117, 2017.

[16] A. Kargermanov, P. Ceresa, 3D Fiber-based frame element with multiaxial stress interaction for RC structures, *Advances in Civil Engineering*, **2018**, https://doi.org/10.1155/2018/8596970, 2018.

[17] Seismosoft, *SeismoArtif v2016*. Available from http://www.seismosoft.com, 2016.

[18] M.J.N. Priestley, G.M. Calvi, M.J. Kowalsky, *Displacement-Based Seismic Design of Structures*. IUSS Press, Pavia, Italy, 2007.

[19] E. Smyrou, T.J. Sullivan, M.J.N. Priestley, G.M. Calvi, Dynamic Behaviour of T-shaped RC Walls Designed with Direct Displacement-based Design. *14th World Conference on Earthquake Engineering*, Beijing, China, 2008.

[20] J.A. Morales, *Seismic Shear and Moment Demands in RC Wall Buildings*. Ph.D Thesis, Istituto Universitario di Studi Superiori di Pavia (IUSS), 2018.

[21] K. Beyer, S. Simonini, R. Constantin, A. Rutenberg, Seismic shear distribution among interconnected cantilever walls of different lengths, *Earthquake Engineering & Structural Dynamics*, **12**, 1423-1441, 2014.